

Growth and morphology of ultrathin Fe films on Cu(001)

J. Giergiel,* J. Shen, J. Woltersdorf, A. Kirilyuk, and J. Kirschner

Max-Planck Institut für Mikrostrukturphysik, Weinberg 2, D-06120 Halle (Saale), Germany

(Received 27 October 1994)

The relationship between magnetism and morphology of pseudomorphic ultrathin films of fcc Fe on Cu(001) is reexamined in view of morphological data obtained with scanning tunneling microscopy. Two types of films showing different magnetic properties were investigated. Films prepared at 300 K are found to grow in a good layer-by-layer mode. Their magnetism appears to be influenced by structural instabilities connected with a martensitic fcc→bcc transformation. Films deposited at 130 K and later annealed at 300 K grow in a Stranski-Krastanov-like mode, resulting in a drastically different surface morphology. They are found to be structurally stable in the region where the spin reorientation takes place. An attempt is made to correlate the enhanced roughness of these films with their magnetic properties. Finally, the connection between the morphological percolation and the onset of long-range ferromagnetic ordering is discussed. The percolation of the first layer is found to be insufficient to establish long-range ferromagnetic ordering in these films.

I. INTRODUCTION

Ultrathin films of iron epitaxially grown on fcc surfaces represent a unique system to study the magnetism of γ Fe (fcc). Provided the misfit is not too large (i.e., within the limits of pseudomorphic growth), epitaxy makes it possible to stabilize the phase which otherwise exists only above 1184 K. Copper(001) is the substrate of choice for pseudomorphic fcc Fe because a small negative misfit ($\approx 1\%$) forces an increased lattice spacing. According to the *ab initio* electronic structure calculations, an increased lattice constant may stabilize a ferromagnetic ground state in the otherwise antiferromagnetic fcc Fe.¹ Furthermore, the magnetic properties of ultrathin films are expected to be different from the magnetism of bulk samples. As shown by Mermin and Wagner² long-range ferromagnetic ordering in two-dimensional systems can be stabilized only by magnetic anisotropies. Moreover, in systems where the surface uniaxial anisotropy favors the perpendicular direction of magnetization, a critical thickness exists where the magnetization rotates into the plane of the film. This unusual transition is often accessible experimentally. It is therefore not surprising that ultrathin films of Fe on Cu(001) have been extensively investigated.³

The system proved, however, to be very complicated. Its magnetic properties strongly depend on the preparation conditions but relatively little has been known about how the preparation conditions affect the growth and morphology of these films. In the following we present extensive morphological investigation of films deposited at different temperatures. We focus on the morphology on the nanometer scale. Clear and distinct differences are observed in films prepared according to two commonly used recipes—low-temperature deposition followed by 300-K anneal, and direct 300-K deposition. This additional morphological information permits a deeper insight into the origin of the magnetic properties of this ultrathin system.

A. Growth and stability considerations

To a certain extent, the feasibility of any epitaxial system can be evaluated by considering the bulk properties of constituent materials. For Fe/Cu the situation is as follows. The bulk miscibility of Cu in both γ and α Fe is small — a few percent at high temperatures (≈ 1200 K) and even less at lower temperatures.⁴ Similar solubility levels are reported for Fe in Cu, but this encouraging picture (sharp interfaces) looks less promising if surface tension data are included. They indicate that copper may segregate to the surface at the initial stages of growth. Existing literature data suggest that some Fe/Cu interface segregation may indeed occur at room temperature (RT).^{5,6} One intuitively expects that lower deposition temperatures should retard this undesired segregation.

Of more direct relevance to the growth mode are the surface and interface free energies. In the first approximation, they determine whether the growth proceeds in the desired layer-by-layer (Frank–Van der Merwe) mode. Reliable data for surface/interface energies are hard to obtain. Nevertheless, the best estimations ($\sigma_{\text{Fe}} > \sigma_{\text{Cu}} + \sigma_{\text{Cu-Fe}}$) indicate⁷ that Fe may prefer to grow in the so-called Volmer-Weber (agglomeration) mode. Below, we will present evidence that this is not the case; the growth of Fe on Cu is primarily determined by kinetic limitations; the thermodynamic equilibrium implicit in simple considerations is very difficult to realize experimentally. A very good example of this difficulty can be seen in the following. According to the energy balance shown above, the system will prefer a sandwich configuration Cu Fe-Cu. As we showed recently,⁷ this indeed is the case but only if a special annealing regime is applied to the system. Under normal conditions (room- or lower-temperature deposition), the system cannot approach this state.

Further complications are expected to arise from the inherent structural instability of Fe films on copper,

which could have two origins. The first one, viz., lattice mismatch, is not expected to be dominant. The best estimation for the lattice constant of antiferromagnetic (or nonmagnetic) γ Fe yields a 1% tensile strain if perfect fit is assumed. Similarly, the ferromagnetic state envisioned by theoretical calculations¹ would result in a 1% compressive strain. Strains of this magnitude are not expected to generate misfit dislocations below 20 ML.⁸ A far stronger instability is due to the fact that at 300 K the fcc phase of iron is some ~ 0.04 eV/atom less favorable than the bcc phase.⁹ The fcc phase normally exists only above 1184 K. There is, therefore, no question that at some thickness the epitaxial registry will no longer be able to provide the fcc phase with sufficient stability and some transformation to the bcc phase should be observed. We will show below that there are some interesting finite size effects connected with this transformation.

B. Previous experimental observations

In view of the above, it is not surprising that the growth of Fe on Cu is experimentally difficult. Much variation is expected with the experimentally accessible range of deposition parameters: flux rate, substrate condition, and temperature. That, indeed, has been the case, and two distinct preparation procedures resulting in films exhibiting different magnetic properties have been identified. In the first procedure, the film is deposited at low temperatures (LT) (< 140 K) and subsequently annealed at ~ 300 K.¹⁰ Alternatively the films are deposited at or slightly above 300 K. We will refer to these two types of films as LT- and RT-deposited films, respectively. Their magnetic properties as reported by Thomassen *et al.*¹¹ and Allenspach and Bischof¹² are shown in Fig. 1. It is immediately clear that the ultrathin films of fcc Fe/Cu(001) are ferromagnetic. However, the exact magnetic behavior strongly depends on the preparation conditions. The two classes of films LT and RT grown only share two common characteristics: (a) the lack of discernible magnetic ordering below 2 ML and (b) the perpendicular anisotropy in the 2–5-ML-thickness range. Above 5 ML thickness their magnetic properties differ. RT-grown films still show a perpendicular anisotropy but with the strongly reduced magnetization, which remains constant up to 10–12 ML. At 10–12 ML, the magnetization rotates into the plane of the film.¹¹ The LT-deposited films undergo a spin-reorientation transition much ear-

lier, i.e., between 5 and 6 ML as can be seen in Fig. 1. Strictly speaking, the behavior in the perpendicular to in-plane transition range (5–6.5 ML) of these LT films is temperature dependent in quite a fascinating way (see Pappas *et al.*¹³).

II. GROWTH KINETICS AND MORPHOLOGY

Since, as discussed above, the growth mode of iron on copper is expected to be strongly temperature dependent it would be quite instructive to reexamine the growth and morphology of these films. The following presents the data that emerged from our recent scanning tunneling microscopy (STM) investigation of this system. Iron films were prepared in an ultrahigh-vacuum chamber with Auger, low/medium-energy electron diffraction (L/MEED), and magneto-optical Kerr effect (MOKE) characterization facilities. STM imaging was performed in a separate chamber with similar capabilities. Iron was evaporated ($\lesssim 0.3$ ML/min) onto the clean and annealed Cu(001). The evaporation was incremental for RT-deposited films (300 K ± 5), and all-at-once for LT films (130 K). The latter were annealed to 300 K before imaging. Particular attention was paid to the quality of the Cu surface. If necessary, the preparation cycle (sputtering and annealing) was repeated until an area with a terrace some 400 nm wide was found within the $5\text{-}\mu\text{m}$ scanning range of the STM. Such a surface was judged sufficiently “flat” for subsequent imaging because the influence of terrace steps on the film growth was determined to be limited to, at most, some 10 nm. Background carbon/oxygen contamination of as-deposited Fe films was estimated to be less than 2 at.%. The coverage calibration was determined by taking STM images at small incremental thickness steps and estimating the area of all visible monatomic levels. The advantage of this rather tedious procedure is that in addition to a good accuracy (0.1–0.2 ML) it yields important information about changes in the film morphology during film growth. The magnetic properties of these films were found identical to those reported in the literature,^{11,12} Fig. 1.

In Figs. 2(a)–2(e), the surface morphology of the LT- and RT-deposited films is compared side-by-side. The first two images [Fig. 2(a)], taken at a 0.4-ML coverage, illustrate the initial stage of growth on an area approximately 100×100 nm.¹⁴ There is a high nucleation density in both cases, but on an average the islands in the LT-

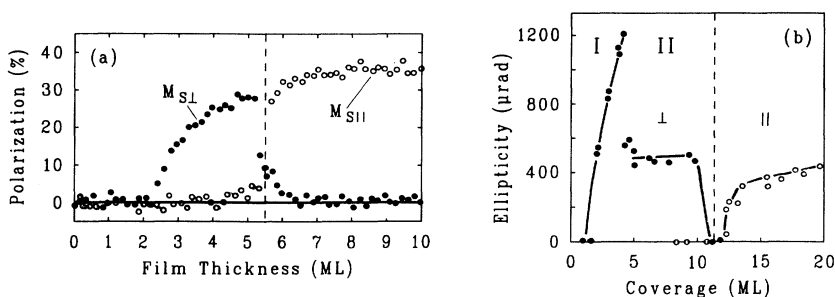


FIG. 1. Magnetic properties of ultrathin films of Fe on Cu(001) prepared at (a) 90 K and (b) room temperature. (a) shows the thickness dependence of the spin polarization of secondary electrons measured at $T=175$ K (after Ref. 12). (b) shows the Kerr ellipticities at saturation measured between 110–400 K and extrapolated to $T=0$ K (after Ref. 11).

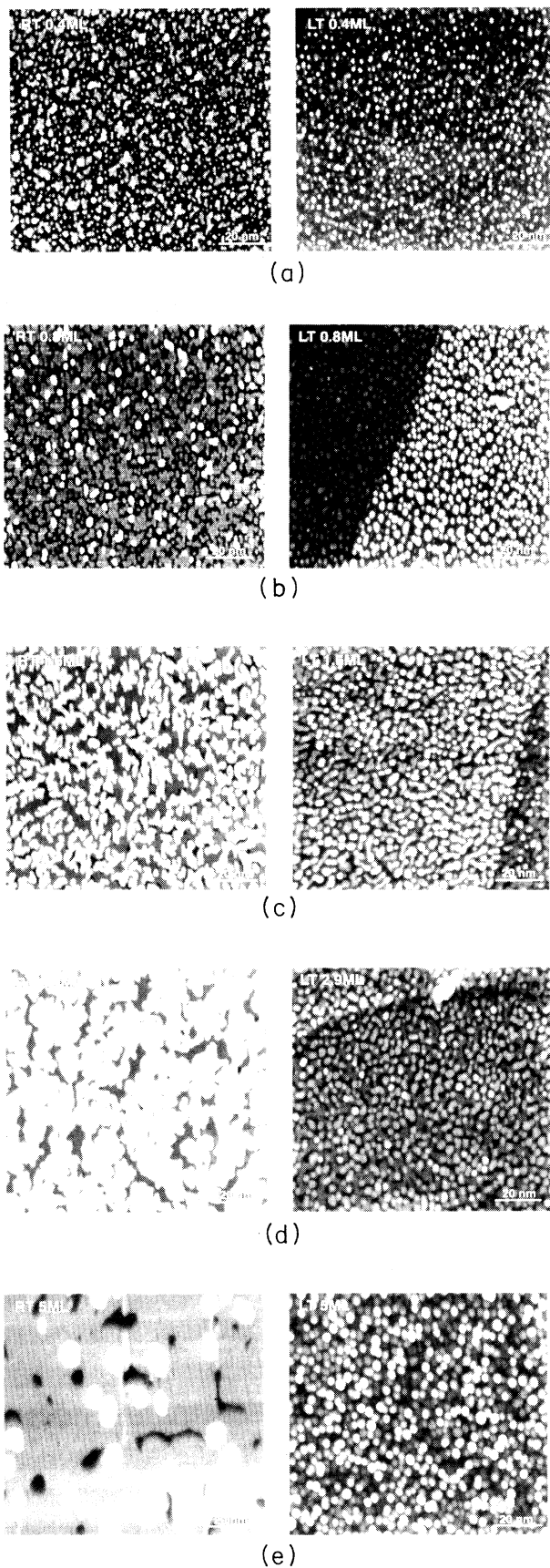


FIG. 2. (a)–(e). The surface topography of Fe films deposited on Cu(001) at room temperature (RT), and at low temperatures ($T \approx 130$ K) and annealed at 300 K (LT). All figures show an area of approximately 100×100 nm imaged with a scanning tunneling microscope operating in a constant current mode with a positive sample bias of 0.6–1 V and a tunneling current of 0.1–0.3 nA. (a) This particular figure shows the topography of 0.4-ML-thick films. A significant part of the original surface remains exposed (darkest gray level). Both first- and second-layer islands (shown progressively whiter) are visible. Note the high nucleation density evident in both room- and low-temperature deposited films. The proportion of second-layer islands is higher in the LT-deposited film. (b) A 0.8-ML-thick film. In the RT-deposited film, the additional 0.4 ML is mostly seen in enlarged first-layer islands, which appear very close to their percolation threshold (0.9 ML). The size of the islands in the LT-deposited film is similar to that of the 0.4-ML film. Consequently, they acquire an almost classical bilayer structure. They will percolate at 1.2 ML. Note that the terrace step visible in the image of the LT-deposited film has no effect on the growth morphology. This is not the case for RT-deposited films (see the text). (c) 1.6-ML-thick films, i.e., films that are on the threshold of establishing the long-range ferromagnetic order ($T_C > 200$ K). The RT-deposited film has already started a stable layer-by-layer growth (there are at most three levels visible at any stage, see also Fig. 5), the mode it will continue from now on. The second layer in the RT film is approaching its percolation threshold (1.7 ML). Some partial coalescence of the original bilayers occurs in the LT-deposited film resulting in a small reduction in the island density. Note the large number of third-layer islands visible in the LT film whereas there are almost none in the RT film. The LT growth begins a Stranski-Krastanov-like growth mode. (d) 2.9-ML-thick films, i.e., films that already show a well-established ferromagnetic ordering. The islands in the RT-deposited film grew much larger while there was no change in the island density of the LT-deposited film. Consequently, the roughness of the LT-deposited film is significantly higher. At a thickness of 3.0 ML, the second LT-film layer will finally percolate. (e) A 5-ML-thick film, i.e., a thickness where major changes in the magnetic properties are occurring. Note the very rough texture of the LT-deposited film, and the appearance of faint, vertical protrusions in the RT film. They are the sites where the martensitic transformation (shown in Fig. 5) starts taking place.

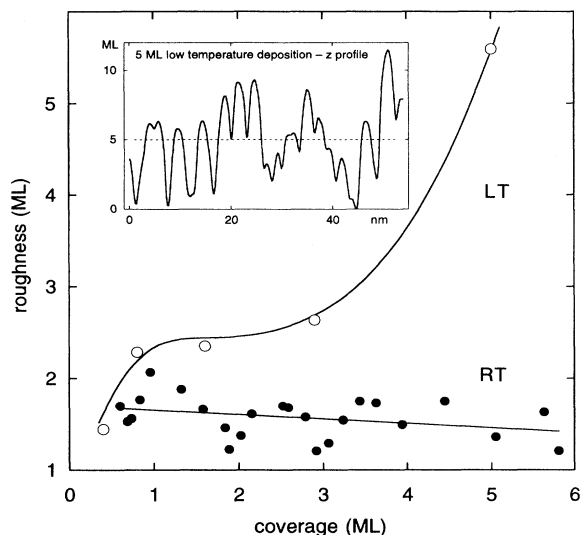


FIG. 3. RMS surface roughness of (RT) Fe films deposited on Cu(001) at room temperature, and (LT) deposited at 130 K and annealed at 300 K. Note the oscillations around the average, slowly decreasing roughness of the RT-deposited films. They indicate the good layer-by-layer growth mode. The strong increase in the roughness of LT films observed between 3 and 5 ML reflects the kinetic limitations of the low-temperature growth. The inset shows a representative profile (height/ML vs distance/nm) of a 5-ML-thick, low-temperature deposited film.

grown film are smaller and the percentage of iron in the second layer (i.e., smaller islands nucleated on top of the first layer and shown in white) is higher. A significant part of the original copper surface (darkest gray level) is still exposed as expected for this coverage.

Figure 2(b) shows the situation for a slightly higher coverage, i.e., at 0.8 ML. The differences between the LT- and RT-grown films are now much more pronounced. A few additional second-layer islands occur in the RT-deposited film indicating that the additional 0.4 ML of iron is still in the first layer islands. On the other hand, the same additional 0.4 ML of iron on the LT-grown film

is in the second layer resulting in an almost classical bi-layer configuration. Consequently, the density of islands is reduced in the RT-grown film and almost unchanged in the LT-grown film. The dramatic differences between LT and RT films are likely due to both thermodynamics and magnetostriction effects as suggested by Ref. 15.

At the coverage of 1.6 ML [Fig. 2(c)] some further changes are obvious. The first layer in the RT-deposited film is well past its percolation¹⁶ threshold (estimated to be 0.9 ± 0.1 ML), but it is still not completed as there are still some openings to the substrate left. Consequently, there are three monatomic levels present: the substrate, and the first and the second Fe layers. The second layer is near its percolation threshold, which is estimated to be 1.7 ± 0.1 ML. The RT growth proceeds from this point on in its layer-by-layer mode (see also Fig. 4). In the LT-deposited film partial coalescence of the original bilayers results in a small reduction in the island density. Note also that the third-layer islands, which are quite numerous in the LT-deposited film, are almost nonexistent in the RT film; that film consists almost entirely of the first and the second Fe layers. A detailed analysis of the LT-deposited film reveals that its first layer is also already percolated (threshold ≈ 1.2 ML).

Going to 2.9 ML changes the morphology a little [Fig. 2(d)]. The islands in RT-grown films tend to grow much larger, while the island density in the LT-deposited film is already frozen-in. Clearly, the interlayer mass transport at 130 K is significantly reduced compared with 300 K. This is reflected in the higher percolation threshold for the second layer observed in these films, i.e., 3 ML versus 1.7 for the RT-grown film.

Similar trends are observed when the thickness is increased from 2.9 ML to 5 ML [Fig. 2(e)]. In the RT-deposited film, the islands become still larger; approaching the transverse correlation length of a typical MEED experiment. This results in a relatively sudden increase in the MEED intensity as can be seen, for example, in Ref. 11. On the other hand, the island density of the LT-grown film does not change much. Consequently, the LT-deposited film acquires a significant roughness at this thickness, the valley to peak amplitude can be as high as 10 ML (≈ 1.8 nm) whereas the characteristic lateral size

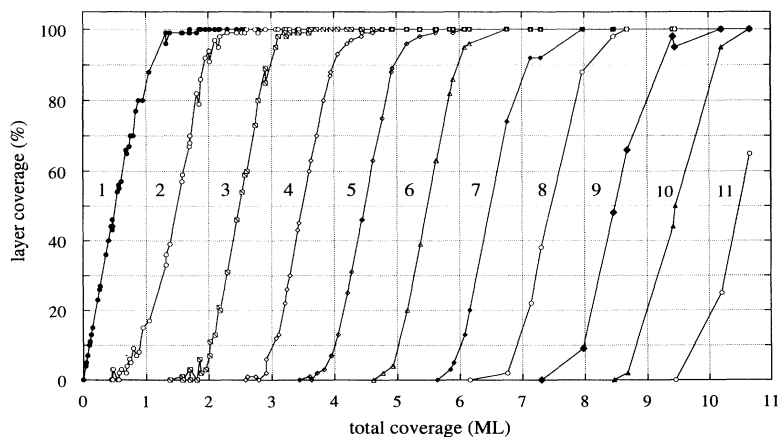


FIG. 4. Layer coverage as a function of total coverage for RT-deposited Fe/Cu(001) films. Note an almost ideal layer-by-layer growth mode throughout the entire thickness range.

of small grains is 3 nm (see the inset in Fig. 3).

The surface roughness of these two films is compared in Fig. 3. For RT-deposited films the roughness tends to oscillate around the average, which slowly decrease with thickness. This behavior of the roughness of RT-evaporated films is consistent with the observed layer-by-layer growth mode of these films where at any time the maximum of three monatomic levels is observed, see Fig. 4. The roughness of the LT-deposited films is initially comparable but quickly becomes much larger than that of the RT-deposited films. At 5 ML, the LT-deposited films are approximately five times rougher.

A closer look at Fig. 2(e) reveals the existence of faint, streaky protrusions in the image of this 5-ML-thick RT-deposited film. These are the sites where the martensitic fcc→bcc transformation starts taking place. The RT-grown film is now thick enough to become unstable. With increasing thickness the transformation progresses quickly, see images in Fig. 5 and a more extensive discussion in Ref. 8. At 10–12 ML, the RT-grown film becomes predominantly bcc with its characteristic surface relief whereas a martensitic product phase (coexistent fcc and bcc phases) of various proportions is present between 5 and 10 ML. No such phase is observed in the LT-grown films (at least up to 10 ML thickness), apparently because it takes some finite lateral size for the fcc phase to become unstable. This is a somewhat unexpected result; the better the film from the morphological standpoint the worse is its structural stability.

III. CORRELATION WITH MAGNETIC PROPERTIES

A. Onset of ferromagnetism and morphological percolation

The onset of ferromagnetic ordering in both types of films is delayed. It has been suggested¹⁷ that this delayed onset of ferromagnetic ordering is due to some kind of magnetic percolation. Clearly, a disconnected collection of nanoscale-sized islands cannot support a long-range ferromagnetic ordering. Some coalescence resulting in percolation paths on the scale of at least a fraction of a micrometer must first take place. Our data suggest that the percolation of the first layer is insufficient to establish the ferromagnetic order. The first layer percolates morphologically long before any ferromagnetic ordering is observed; the percolation threshold is 0.9 and 1.2 ML for RT- and LT-deposited films, respectively,¹⁸ while the experimentally observed ferromagnetic onsets are ≈ 2.1 ML for the LT-deposited films,¹² and at ≈ 1.7 ML for the RT-deposited films (Fig. 1).^{11,19} This inability of the system to establish ferromagnetic ordering at its percolation threshold is in strong contrast to the recently reported observation of the percolation/coalescence induced transformation from the superparamagnetic to the ferromagnetic behavior in bcc Fe *submonolayer* on W(110).²⁰ Instead, the ordering appears at 1.7 ML in RT-deposited films, i.e., at the point where the second layer of this film

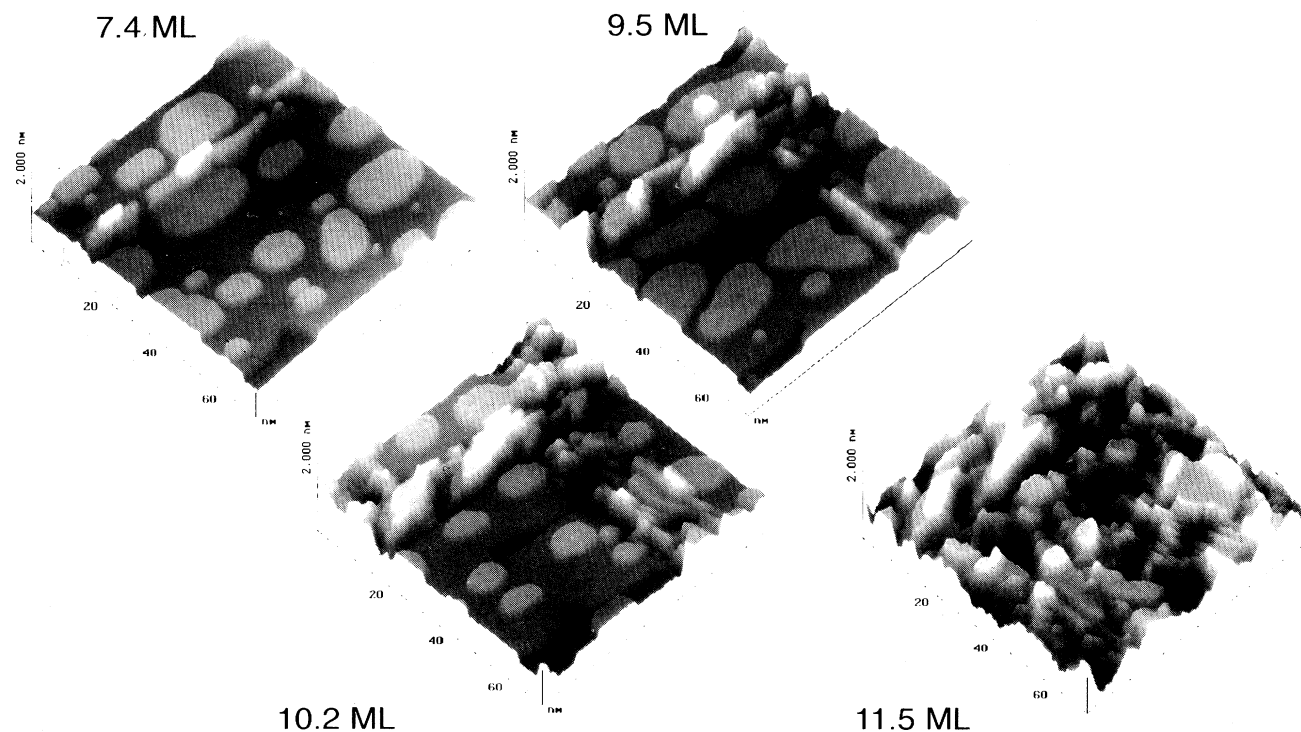


FIG. 5. A series of STM images showing the evolution of the surface morphology of a RT-deposited film as a function of film thickness. One particular 70×70 -nm area of the sample is depicted. Note the gradual increase in the area occupied by bcc precipitates at the expense of the original fcc phase. At 11.5 ML, the film is entirely converted into bcc resulting in an extremely rough surface texture owing to a large mismatch of this Fe phase with the Cu substrate.

percolates. The LT-deposited films order magnetically¹² at ≈ 2.1 , i.e., below the second-layer percolation threshold (3 ML).

There could be several reasons for this delayed onset of ferromagnetism in the Fe/Cu(001) system. The first layer might be intermixed with copper. Such intermixing has been often reported for RT-deposited films, see, e.g., Refs. 21 and 22. However, intermixing is expected to be significantly retarded in films prepared at low temperatures, but, as pointed out above, even these films do not show ferromagnetic ordering at their first-layer percolation threshold. Moreover, recent results on metastable FeCu alloys indicate that even severe intermixing has little effect on magnetic properties of Fe.²³ The nearest-neighbor distance is 2.55 Å as compared to 2.73 Å in the Fe/W(100) system. Comparable variation of the lattice constant of bulk fcc Fe results in major changes in its magnetic properties, see Moruzzi *et al.*¹ Furthermore, the reduced symmetry of the bcc(110) surface provides a strong uniaxial in-plane anisotropy that may be responsible for stabilizing the magnetism at lower thicknesses.²⁰ And, last, the coordination of surface atoms is different in both systems, which could lead to different hybridization effects.

B. Magnetic properties of Fe films deposited at low temperatures

In the 2–5-ML-thickness range both classes of films are fcc or slight modifications thereof [LEED, surface-extended x-ray absorption fine-structure (SEXAFS) data of Refs. 24 and 25]. Both show a ferromagnetic ordering with a saturation magnetization following the expected thickness dependence. The magnetization direction is perpendicular to the plane of the film indicating that the uniaxial surface/interface anisotropies preferring such orientation is present. The magnetization switches later in-plane. It is not certain, however, whether the expected $1/d$ switching mechanism holds here exactly. The reason is that with increasing thickness we also see major changes in the surface morphology (Fig. 3). It is doubtful whether a surface that is as rough as that seen in 5–6 ML, LT-deposited films can be characterized by the same uniaxial surface anisotropy as is applicable to smooth films. The roughness on this scale must significantly affect its anisotropy. We therefore conclude that the magnetization reversal observed in 5–6 ML, LT-deposited films is likely to be driven by both the increase in the effective macroscopic shape anisotropy and by a roughness-induced modification of the effective uniaxial surface term.

Further consequences of the increased surface roughness are expected to occur in the domain structure of these films. Recall that the domain formation is governed by the balance between magnetostatic and domain wall energies. The domain wall widths in this system are estimated to be much less than 20 nm (Ref. 17) and, thus, approaching the characteristic size of grains in LT films (3 nm). If the domain wall width is comparable with

grain sizes, a significant modification of domain wall energies should follow. That this might be the case here can be seen from the dramatic differences observed between characteristic domain sizes in 2.8-ML RT- and LT-deposited films [close to our 2.9 ML film that is shown in Fig. 2(d)]. They are two orders of magnitude different, 1 μm and 100 μm , respectively, as reported by Allenspach.¹⁷

C. Magnetic properties of Fe films deposited at 300 K

1. Transition in the 4–5-ML-thickness range

At 4–5 ML thickness where the LT-deposited films show the transition from perpendicular to in-plane magnetization, the RT-deposited films show quite a different behavior (Fig. 1). The saturation magnetization suddenly drops but its direction remains the same. In addition, the saturation magnetization remains constant throughout the entire 5–10-ML range. This surprising result was interpreted in terms of magnetic live surface layers.¹¹ More recently Li *et al.*¹⁵ reported that the initially constant saturation magnetization develops a small temperature-dependent modulation below 200 K. They interpret this as a manifestation of antiferromagnetic ordering in layers below the two topmost ferromagnetic layers.

It has been suggested that some structural transformation in these RT-deposited films is responsible for the observed magnetic behavior change at 4–5 ML. According to SEXAFS studies, thin films are in a tetragonally distorted state²⁴ whereas thicker films assume a more perfect fcc structure. Similar conclusions have been drawn in a quantitative LEED analysis of Müller *et al.*²⁵ The exact nature of this transformation has not yet been elucidated. Our data indicate that we may be seeing this structural transformation. Note that 4–5 ML is the thickness where RT-grown films are already sufficiently contiguous and thick enough to become unstable toward a fcc \rightarrow bcc transformation. As shown in Figs. 2(e) and 5, and as discussed in detail in Ref. 8, the transformation proceeds by nucleation of a network of thin dislocation-like needles, which later on develop into characteristic martensitic bcc needles (grains). It is plausible that these grains relax their parent fcc phase. Since for most of the 5–10-ML range the bcc phase remains negligible in terms of the fractional it occupies, the magnetic response measured by area integrating techniques is that of the “relaxed” fcc parent phase.

2. Transition in the 10–12-ML-thickness range

As a final note, we would like to comment on a magnetic transition observed in the RT-grown films at still higher thicknesses. As shown in Fig. 1, at 10–12 ML the magnetization switches to the in-plane orientation and the entire film becomes magnetic again. This is not the

same switching as that observed at 5 ML in LT-deposited films where the shape and surface/interface anisotropies drive the switching. At 10–12 ML, the RT-grown film is becoming predominantly bcc and the magnetism reflects the properties of this new phase. This already has been appreciated for some time,²⁶ and is additionally confirmed by our most recent work.²⁷ By following a special preparation procedure, we are now able to prepare γ -Fe films that are perfectly stable up to 60 ML. Preliminary magnetic data of these stabilized films clearly show that the thick γ -Fe films (> 10 ML) are nonferromagnetic ($T_C < 200$ K) provided the precipitation of the bcc phase can be avoided.

IV. CONCLUSIONS

The primary finding that emerges from the morphological data presented here is that the magnetic behavior of RT-deposited Fe film is significantly influenced by its structural instability. It is quite ironic than, that the consequences of the competition between surface and volume shape anisotropies, i.e., the anisotropy driven spin reorientation, is observed in structurally much less perfect LT-grown films and not in the RT-grown films that grow

in a much better layer-by-layer mode. The morphology of these LT-deposited films has important consequences from both the structural and magnetic point of view. It stabilizes the ferromagnetic phase of fcc iron at higher thicknesses, making it possible to observe the magnetization direction reorientation transition, which in RT-deposited films seem to be obscured by the martensitic fcc \rightarrow bcc transformation. Furthermore, it is expected to influence the delicate balance between the shape and the uniaxial surface anisotropies, which drive this transition, and to affect the domain behavior of these films to a significant degree. The intuitively tempting picture of a close connection between the morphological percolation of the first layer and the onset of ferromagnetism is clearly not applicable to this system. Future investigations are necessary to clarify the reasons for the delayed onset of ferromagnetism observed in these epitaxial films.

ACKNOWLEDGMENTS

The authors would like to thank R. Allenspach and M. Wuttig for the permission to reproduce their data in this article (Fig. 1).

* Author to whom correspondence should be addressed.

¹ V. L. Moruzzi, P. M. Markus, and J. Kübler, *Phys. Rev. B* **39**, 6957 (1989).

² N. D. Mermin and H. Wagner, *Phys. Rev. Lett.* **17**, 1133 (1966).

³ It is impractical to cite here all the relevant publications. See Refs. 5–8, 10–13, 15, 16, 19, and 20, 22–25, and citations therein.

⁴ W. B. Pearson, *A Handbook of Lattice Spacings and Structures of Metals and Alloys* (Pergamon, New York, 1958).

⁵ M. T. Kief and W. F. Egelhoff, Jr., *J. Vac. Sci. Technol. A* **11**, 1661 (1993).

⁶ D. D. Chambliss, K. E. Johnson, R. J. Wilson, and S. Chiang, *J. Magn. Magn. Mater.* **121-122**, 1 (1993).

⁷ J. Shen, J. Giergiel, A. Schmid, and J. Kirschner, *Surf. Sci.* **328**, 32 (1995).

⁸ J. Giergiel, J. Kirschner, J. Landgraf, J. Shen, and J. Woltersdorf, *Surf. Sci.* **310**, 1 (1994).

⁹ K. S. Cheung, R. J. Harrison, and S. Yip, *J. Appl. Phys.* **71**, 4009 (1992).

¹⁰ D. A. Steigerwald, I. Jacob, and W. F. Egelhoff, Jr., *Surf. Sci.* **202**, 472 (1988).

¹¹ J. Thomassen, F. May, B. Feldmann, M. Wuttig, and H. Ibach, *Phys. Rev. Lett.* **69**, 3831 (1992).

¹² R. Allenspach and A. Bischof, *Phys. Rev. Lett.* **69**, 3385 (1992).

¹³ D. P. Pappas, K. P. Kämper, and H. Hopster, *Phys. Rev. Lett.* **64**, 3179 (1990).

¹⁴ The aspect ratios may be less than ideal due to inherent difficulties in compensating fast and slow scanning direction drifts.

¹⁵ Dongqi Li, M. Freitag, J. Pearson, Z. Q. Qiu, and S. Bader, *Phys. Rev. Lett.* **72**, 3112 (1994).

¹⁶ Percolation as mathematically defined (finite probability of an infinite path) cannot be tested in our system. Instead, we use an operational definition—90% of islands of a given height must be interconnected on a representative 25×25 -nm area before they are considered percolated.

¹⁷ R. Allenspach, *J. Magn. Magn. Mater.* **129**, 160 (1994).

¹⁸ It is unlikely that the well-known finite thickness scaling of T_C —R. Bergholz and U. Gradmann, *J. Magn. Magn. Mater.* **45**, 389 (1984)—prevents the observation of ferromagnetic ordering in thinner films. Even at the lowest thickness where the ferromagnetic ordering is first observed (1.7 ML), the T_C is already well above room temperature, Ref. 11. At least some thinner films should show ferromagnetic ordering within the experimentally accessible temperature range.

¹⁹ D. Pescia, M. Stambanoni, G. L. Bona, A. Vaterlaus, R. F. Willis, and F. Meier, *Phys. Rev. Lett.* **58**, 2126 (1987).

²⁰ H. J. Elmers, H. Hauschild, H. Höche, U. Gradmann, H. Bethge, D. Heuer, and U. Köhler, *Phys. Rev. Lett.* **73**, 898 (1994).

²¹ K. E. Johnson, D. D. Chambliss, R. J. Wilson, and S. Chiang, *Surf. Sci.* **313**, L811 (1994).

²² N. Memmel and T. Detzel, *Surf. Sci.* **307**, 490 (1994).

²³ P. A. Serena and N. Garcia, *Phys. Rev. B* **50**, 944 (1994).

²⁴ H. Magnan, D. Chandresris, B. Vilette, O. Heckmann, and J. Lecante, *Phys. Rev. Lett.* **67**, 859 (1991).

²⁵ S. Müller, P. Bayer, C. Reischl, K. Heinz, B. Feldmann, H. Zillgen, and M. Wuttig, *Phys. Rev. Lett.* **74**, 765 (1995).

²⁶ P. Xhonneux and E. Courtens, *Phys. Rev. B* **46**, 556 (1992).

²⁷ A. Kirilyuk, J. Giergiel, J. Shen, and J. Kirschner (unpublished).

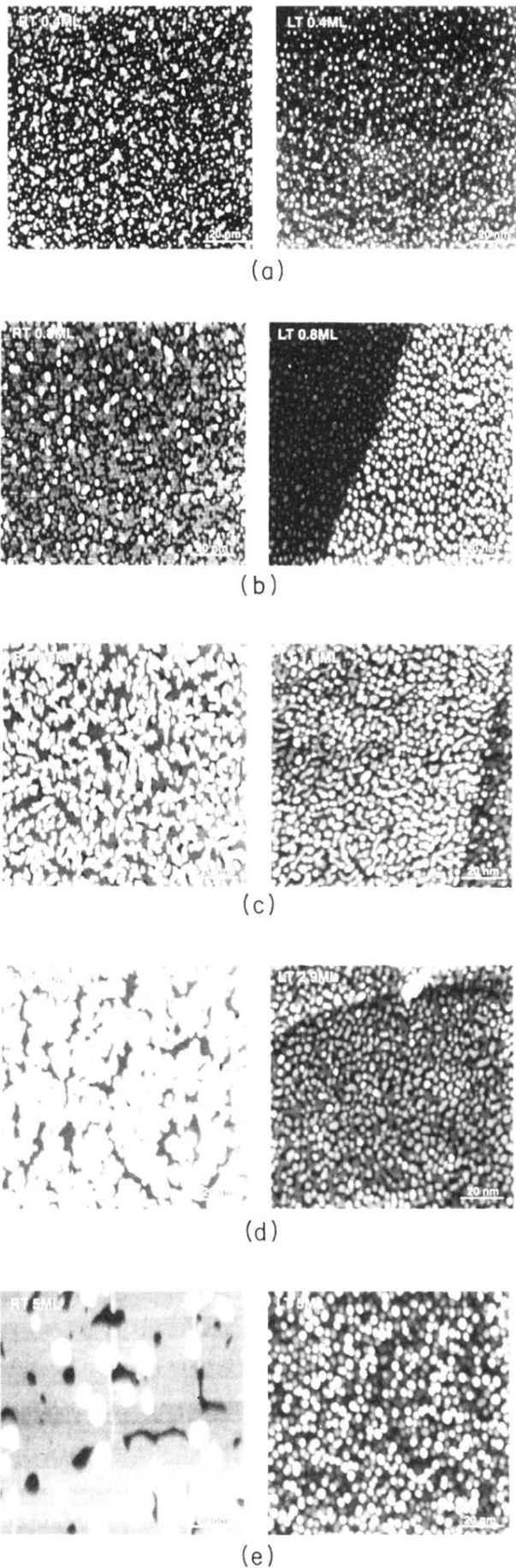


FIG. 2. (a)–(e). The surface topography of Fe films deposited on Cu(001) at room temperature (RT), and at low temperatures ($T \approx 130$ K) and annealed at 300 K (LT). All figures show an area of approximately 100×100 nm imaged with a scanning tunneling microscope operating in a constant current mode with a positive sample bias of 0.6–1 V and a tunneling current of 0.1–0.3 nA. (a) This particular figure shows the topography of 0.4-ML-thick films. A significant part of the original surface remains exposed (darkest gray level). Both first- and second-layer islands (shown progressively whiter) are visible. Note the high nucleation density evident in both room- and low-temperature deposited films. The proportion of second-layer islands is higher in the LT-deposited film. (b) A 0.8-ML-thick film. In the RT-deposited film, the additional 0.4 ML is mostly seen in enlarged first-layer islands, which appear very close to their percolation threshold (0.9 ML). The size of the islands in the LT-deposited film is similar to that of the 0.4-ML film. Consequently, they acquire an almost classical bilayer structure. They will percolate at 1.2 ML. Note that the terrace step visible in the image of the LT-deposited film has no effect on the growth morphology. This is not the case for RT-deposited films (see the text). (c) 1.6-ML-thick films, i.e., films that are on the threshold of establishing the long-range ferromagnetic order ($T_C > 200$ K). The RT-deposited film has already started a stable layer-by-layer growth (there are at most three levels visible at any stage, see also Fig. 5), the mode it will continue from now on. The second layer in the RT film is approaching its percolation threshold (1.7 ML). Some partial coalescence of the original bilayers occurs in the LT-deposited film resulting in a small reduction in the island density. Note the large number of third-layer islands visible in the LT film whereas there are almost none in the RT film. The LT growth begins a Stranski-Krastanov-like growth mode. (d) 2.9-ML-thick films, i.e., films that already show a well-established ferromagnetic ordering. The islands in the RT-deposited film grew much larger while there was no change in the island density of the LT-deposited film. Consequently, the roughness of the LT-deposited film is significantly higher. At a thickness of 3.0 ML, the second LT-film layer will finally percolate. (e) A 5-ML-thick film, i.e., a thickness where major changes in the magnetic properties are occurring. Note the very rough texture of the LT-deposited film, and the appearance of faint, vertical protrusions in the RT film. They are the sites where the martensitic transformation (shown in Fig. 5) starts taking place.

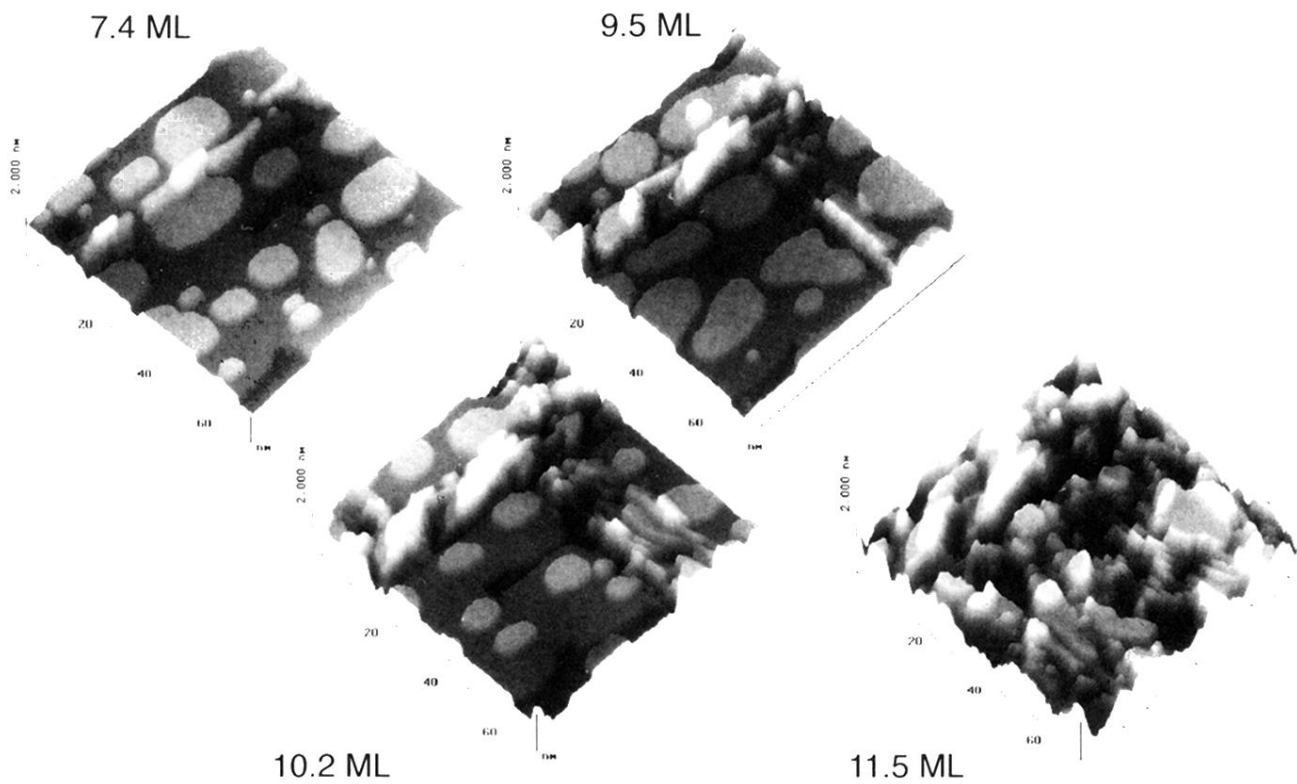


FIG. 5. A series of STM images showing the evolution of the surface morphology of a RT-deposited film as a function of film thickness. One particular 70×70 -nm area of the sample is depicted. Note the gradual increase in the area occupied by bcc precipitates at the expense of the original fcc phase. At 11.5 ML, the film is entirely converted into bcc resulting in an extremely rough surface texture owing to a large mismatch of this Fe phase with the Cu substrate.